Journal of Non-Crystalline Solids 387 (2014) 1–5

Contents lists available at ScienceDirect

Journal of Non-Crystalline Solids

journal homepage: www.elsevier.com/ locate/ jnoncrysol

Buckling of metallic glass bars

J.G. Wang [a,b], K.C. Chan [b,*], J.C. Fan [a], L. Xia [c], G. Wang [c], W.H. Wang [d]

[a] School of Materials Science and Engineering, Anhui University of Technology, Ma'anshan, 243002, China
[b] Advanced Manufacturing Technology Research Centre, Department of Industrial and Systems Engineering, The Hong Kong Polytechnic University, Hung Hom, Hong Kong
[c] Laboratory for Microstructures, Shanghai University, Shanghai 200444, China
[d] Institue of Physics, Chinese Academy of Sciences, Beijing 100190, China

ARTICLE INFO

Article history:
Received 24 October 2013
Received in revised form 11 December 2013
Available online xxxx

Keywords:
Buckling;
Metallic glass;
Slenderness ratio;
Shear band

ABSTRACT

Uniaxial compression tests of slender metallic glass bars of composition $Zr_{52.5}Cu_{17.9}Ni_{14.6}Al_{10}Ti_5$ (at.%) have been conducted. It was found that the Zr-based metallic glass bars have a tendency to buckle elastically or plastically rather than to yield or fracture if its slenderness ratio is over a critical value. The elastic buckling undermines the intrinsic strength of the metallic glass, but the plastic buckling imparts the metallic glass a benign failure mode and avoids the catastrophic brittle fracture. The phenomena are understood by the unique stress state across the bar. The result has implication for the measurement of mechanical properties of bulk metallic glasses and is of significance in the application of metallic glass members in engineering structures.

1. Introduction

Due to the lack of tensile ductility at room temperature, bulk metallic glasses (BMGs) and their derivatives, as potential structural material with high strength and good elasticity, are usually tested in uniaxial compression to determine the mechanical properties [1–4]. Rod shaped BMG specimens for compression test generally have an aspect ratio (i.e. height/diameter) of 2 as recommended by ASTM [3]. The aspect ratio is often deliberately reduced [5], sometimes even below unit, to explore the size dependence of the strength and plasticity. In sharp contrast, there are, to date, sparse reports on the compressive performance of BMGs with high aspect ratios, e.g. 3 or above. For a BMG specimen with a constant diameter, a lower aspect ratio actually means a smaller specimen volume which contains fewer flaws, such as pores, microcracks etc. that are induced during the casting and machining process [6]. It alleviates the detrimental influence of the flaws on the inherent mechanical properties of BMGs. On the other hand, once yielding occurs, most BMGs are very prone to localize the plastic strains in the shear bands [1]. Since elastic strain energy is stored inside loaded specimen, the bands in a long BMG rod is more likely to shear in a runaway manner than in a short one, because the energy needed to dissipate per unit area in the shear plane is proportional to the length [6]. This favors short (i.e. low aspect ratio) specimens by virtue of the structure stability. However, the slender members, such as columns, beams and bars, are inevitably employed in engineering structures [7]. More importantly, a slender specimen is different from a stubby one in terms of the failure mode. A bar that is sufficiently slender will buckle rather than yield or fracture under a compressive load [7,8]. For BMGs, the deforming characteristics of slender samples have not received any attention and therefore remain unexplored [1,9].

According to the conventional Euler buckling model [7], the critical stress, σ_E, for a slender bar of a length, l, is

$$\sigma_E = \frac{\pi^2}{(kl/r)^2}E \tag{1}$$

where E is Young's modulus, r is the smallest radius of inertia of the cross section, and k is a dimensionless factor depending on the end restraints. The ratio l/r is called the slenderness ratio (SR) that scales with the aspect ratio. For BMGs, Young's modulus is about 30% smaller than that for the corresponding crystals, and the elastic limit is about twice that for a crystalline material [1,10]. From Eq. (1), it can be concluded that metallic glass is more likely to buckle than its crystalline counterpart with the same end constraints and SR when compressed [4]. Nevertheless, if σ_E exceeds the yield stress, σ_y, of the material, the specimen will yield first and then deform plastically or fracture before the buckling has a chance to intervene. For instance, the σ_E value of a BMG column with the most common aspect ratio of 2 (i.e. SR of 8) and two clamped ends (i.e. k of 0.5) is ~$0.62E$ according to Eq. (1), about 31 times as large as the yield stress, σ_y (~$0.02E$). Thus, BMG samples tested by compression, reported in the literatures, usually yield rather than buckle [1]. Recently, Demetrious et al. [4,11] examined the yield behavior and strength of amorphous Pd-based foams, and they found that the buckling of the intracellular membranes played a vital role in the foam deformation. However, the dimensions of the membrane were on the order of tens of microns, even smaller than the plastic zone thickness in BMGs. Furthermore, there are so many membrane struts in the foam that it is impossible to identify the exact behavior of a single strut despite understanding the foam's overall performance.

* Corresponding author. Tel.: +852 27664981.
E-mail address: kc.chan@polyu.edu.hk (K.C. Chan).

0022-3093/$ – see front matter © 2013 Elsevier B.V. All rights reserved.
http://dx.doi.org/10.1016/j.jnoncrysol.2013.12.008

In this paper, we report the deforming behavior and failure mode of slender Zr-based BMG specimens. Elastic buckling and plastic buckling are both observed in uniaxial compression experiments. We emphasize that the failure mode of the Zr-based BMG buckles rather than yields when the SR increases. A unique manner of shear band development during the buckling is witnessed, which is attributed to the stress gradient across the specimen. Based on the performance of slender BMG bars, the buckling, compared to the catastrophic shearing-off or brittle fracture, is considered to be a more benign failure mode.

2. Experimental methods

Alloy ingots with nominal composition of $Zr_{52.5}Cu_{17.9}Ni_{14.6}Al_{10}Ti_5$ (at.%) were prepared by arc-melting high purity metals under a Ti-gettered purified argon atmosphere, which was then suction-cast into a plate form with dimensions of 70 mm × 12 mm × 1.6 mm in a water-cooled copper mold. Its glassy nature was ascertained by the x-ray diffraction (XRD) technique. The plate was cut into bar shaped specimens for the compression tests. All the specimens were carefully machined and polished to eliminate the surface flaws, and more importantly, to ensure the top and bottom ends were flat and as parallel as possible to each other, and were perpendicular to the longitude loading axial. Uniaxial compression tests were conducted at a strain rate about 10^{-4} s^{-1} at room temperature. The specimens undergoing plastic buckling were observed by scanning electron microscope (SEM) to investigate the features of the developed shear bands in detail.

The dimensions, SRs and σ_Es for the elastic buckling of the specimens are listed in Table 1. As $r = \sqrt{I/A}$ in which I is the smallest area moment of inertia and A is the area of the cross section [7], the SR can be readily calculated. The σ_E value is obtained with an E of 88.6 GPa [10,12], and $k = 0.5$ and 0.7 which correspond to the fixed–fixed end restraint and fixed–pinned end restraint, respectively.

3. Results and discussion

3.1. The issue of plasticity in BMGs

Although extensive efforts have been made to improve the plasticity of BMGs, the experimental data on the plasticity are extremely scattered, sometimes even contradictory [2,3,13–18]. For most Zr-based BMGs, there are two typical ways for the shear band development in the same specimen, as shown in Fig. 1 [13,18]. If the first primary shear band forms in the bottom corner (see Fig. 1a), the upper part of the specimen can slide along this primary shear band, and the capacity loss of load, caused by the reduction of the effective load-bearing area (the red line in Fig. 1), can be duly compensated by the support from the tip P touching the platen. The first primary shear band is stopped and the second one is initiated and develops in a similar way, and the process will continually repeat itself [18]. In this way, "plasticity" is obtained. Conversely, if the first primary shear band forms in the middle of the specimen (see Fig. 1b), the load capacity cannot be compensated immediately by the P' support, and will drop dramatically in the ensuing deformation. Eventually, the specimen is sheared off prematurely and shows poor plasticity.

Table 1
Summary of the dimensions, SRs and σ_Es ($k = 0.5$, fixed–fixed; k = 0.7, fixed–pinned; E = 88.6 GPa) of $Zr_{52.5}Cu_{17.9}Ni_{14.6}Al_{10}Ti_5$ specimens.

No.	Length (mm)	Width (mm)	Thickness (mm)	SR	σ_E (GPa)	
					k = 0.5	k = 0.7
A1	4.50	1.08	0.82	19.0	9.68	4.94
A2	4.52	1.08	0.82	19.1	9.59	4.89
B1	11.39	1.54	0.68	58.0	1.04	0.53
B2	10.84	1.54	0.68	55.2	1.15	0.59
B3	8.44	1.03	0.58	50.4	1.37	0.70
B4	7.00	0.93	0.49	49.5	1.43	0.73
C1	9.16	0.98	0.72	44.1	1.79	0.92
C2	9.08	1.53	0.96	32.8	3.25	1.66
C3	10.46	1.50	1.47	24.6	5.78	2.94
C4	4.79	1.44	0.78	21.3	7.71	3.93

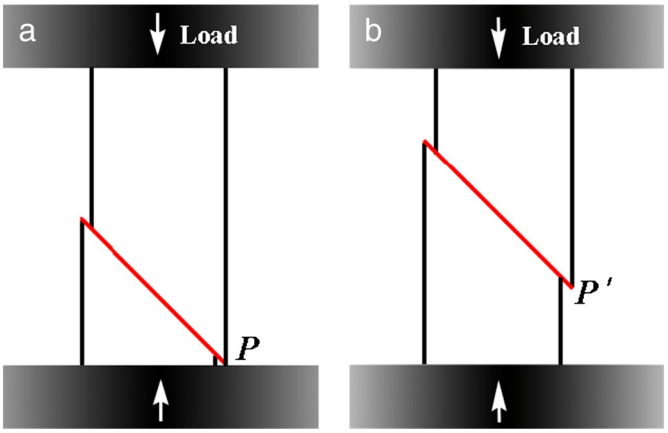

Fig. 1. Schematic of two typical ways for shear band development in a Zr-based BMG. (a) The first primary shear band forms at the bottom corner of the sample. (b) The first primary shear band forms in the middle of the sample.

Fig. 2a shows two stress–strain curves for specimens A1 and A2 with similar dimensions. A1 is sheared off after only about 0.2% plastic strain, whereas A2 sustains more than 0.6% plastic strain without fracture.

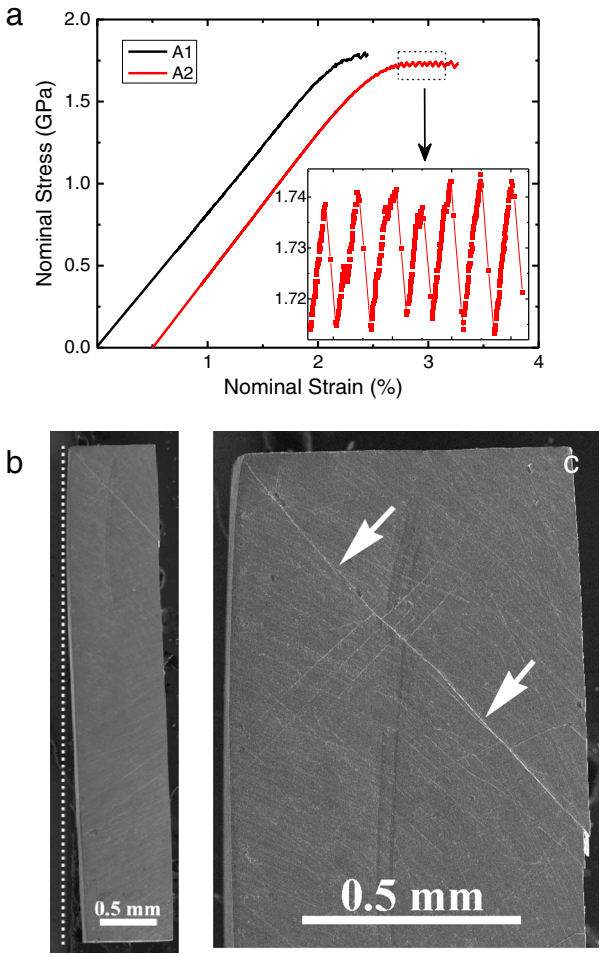

Fig. 2. Investigation on the deformation behavior of stubby samples A1 and A2. (a) Strain–stress curves of A1 and A2 in compression. The inset shows the regular serrations in the plastic deformation regime of A2. (b) A SEM profile of A2 whose top part is magnified in (c).

Fig. 2b shows an overall image of the deformed specimen A2. Obviously, A2 is not sheared off and just has a slight tilt. Fig. 2c exhibits the magnified top part of A2, which clearly shows a primary shear band in the diagonal direction, as marked by the two arrows. Furthermore, regular serrations (see the inset in Fig. 2a) are observed in the plastic deformation of A2, which corresponds to the intermittent sliding along a single shear band [13]. It's just the mode depicted in Fig. 1a. Although the stress–strain relationship leads to the belief that A2 is more plastic than A1, they are actually all the same. In other words, the plasticity in BMGs involves random events as illustrated in Fig. 1, not entirely attributed to the material (intrinsic property and extrinsic geometry) and testing machine [19,20], which has been described by the Weibull distribution [3,17,21].

On the contrary, the results of the bending deflections in BMGs are much less scattered [2,22,23]. This is because there is a neutral plane in the beam, which prevents the primary shear bands from propagating across the specimen due to the low stress level and makes the deflection progress in a stable fashion [24]. Similarly, in a buckled bar exists the stress gradient which can be taken advantage of to arrest the shear bands [7].

3.2. Elastic buckling

Since the yield stress σ_y is ~$0.02E$ in BMGs, the critical SR of a BMG bar for elastic buckling is 44.4 (31.7) according to Eq. (1) when k is taken to be 0.5 (0.7). A1 and A2 with SR values of 19.0 and 19.1, respectively, yield at ~1.75 GPa, and never experience buckling. When the SR goes up to 58.0, σ_E decreases down to far below the yield stress. In this case, the deformation path of B1 deviates into the horizontal at 0.87 GPa, as shown in Fig. 3a. Once unloaded, B1 returns to the initial straightness, suggesting B1 undergo elastic buckling [7,8]. The calculated stress, σ_E, for B1 is 1.04 GPa ($k = 0.5$) as listed in Table 1, which is 0.17 GPa larger than the measured value. In fact, the instant Young's modulus E_i of 76.8 GPa is obtained by linear fitting the elastic region of the deformation. If E is replaced by E_i in Eq. (1), the σ_E is 0.90 GPa, very close to the experimental value 0.87 GPa. Subsequently, B1 is shortened to B2 with a lower SR of 55.2, and its stress–strain relationship is given by the red curve in Fig. 3a. B2 also buckles elastically, but the σ_E increases up to 1.03 GPa, equal to the value predicted by Eq. (1), with E_i of 79.7 GPa and approaching the calculated value of 1.15 GPa in Table 1. Clearly, σ_E is enhanced by reducing the SR. However, if the end constraint is changed, say, from fixed–fixed ($k = 0.5$) to fixed–pinned ($k = 0.7$), σ_E will decrease, even though the SR is lowered as indicated in Eq. (1). B3 with a SR of 50.4 is compressed under the fixed–pinned end constraint, and it buckles at 0.76 GPa, slightly larger than the predicted in Table 1. Then the compression is continued until the stress drops to 0.6 GPa, and no break or snap occurs. The profile of the deformed specimen B3 is shown in Fig. 3b. Apparently, B3 fails by plastic deflection. Meanwhile, no evident serrations appear in the plastic region of the stress–strain curve, which indicates the sliding along a single shear band does not occur. It is confirmed by the SEM observation on the region enclosed by the dotted line in Fig. 3b. Fig. 3c and d exhibit

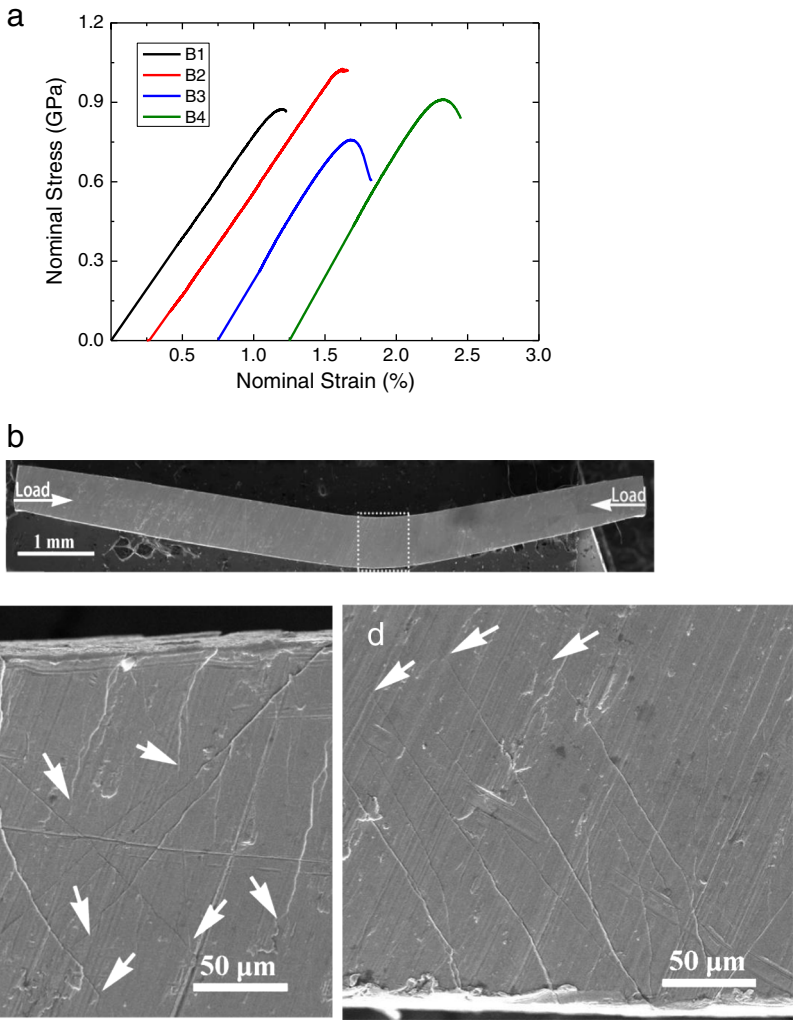

Fig. 3. Elastic buckling behavior of four slender samples with an SR in excess of 44.4. (a) The nominal stress–strain curves for the samples in compression tests. (b) The overall SEM image of the buckled B3. Observation of shear bands on the compression side (c) and tension side (d).

the compression and tension sides, respectively. One can see a number of shear bands are formed on both sides but are terminated around the middle of the bar as marked by the arrows, similar to the morphology of bended BMG specimen [22,23]. Another specimen B4, with an SR almost the same as that of B3, is compressed under a condition of the pinned end with a more flexible constraint as compared with the case in B3. The σ_E rises to 0.91 GPa (see Fig. 3a), but is still only about half the value of σ_y. As such, slender BMG specimens tend to buckle rather than yield under a compressive load. Although it, compared with shearing-off or brittle fracture, is less catastrophic, the strength, determined by σ_E instead of σ_y, is depressed.

3.3. Plastic buckling

To maximize the strength advantage of the BMG, the SR is further reduced. As discussed above, when the SR is below 44.4, the BMG bar cannot buckle elastically under a compressive load if its two ends are clamped. When specimen C1 with an SR of 44.1 is compressed, although its two ends are constrained in an identical way to those for B1 and B2, it still buckles at 0.99 GPa as shown in Fig. 4a (black curve). The stress is close to the elastic buckling stress of 0.92 GPa predicted by Eq. (1), with $k = 0.7$ corresponding to the fixed–pinned end constraint. Fig. 4b shows the profile of the lateral-deflected C1. The nonsymmetrical deformation of the end infers that the fixed end has turned into a half-pinned and half-fixed end to facilitate the buckling. In fact, the SR (44.1) of C1 is greater than the critical SR (31.7) for the fixed–pinned ends, which builds the fundamental basis for the buckling. The SR for C2 is reduced to 32.8, and the corresponding σ_E is 3.25 GPa for fixed–fixed ends and 1.66 GPa for fixed–pinned ends. In compression testing, C2 buckles at ~1.5 GPa, as shown in Fig. 4a (blue curve). An overall image of the deformed C2 is shown in Fig. 4b. One can see that both ends are undoubtedly fixed, unlike the case for C1. Apparently, C2 experiences plastic buckling. On the theoretical side, the bar cannot buckle plastically before yielding. However, flaws, such as pores and inclusions, and the initial crookedness usually result in the stress concentration that causes a local plastic deformation. Once plastic deformation is involved, the E in Eq. (1) should be replaced by the tangent modulus E_t according to Shanley's model [7]. E_t, as a function of the stress level, converts Eq. (1) into a transcendental equation [8]. As a result, the plastic buckling stress, σ_P, has to be obtained by iteration. A σ_P of 1.45 GPa is obtained for C2 with an E_t of 39.7 GPa. Meanwhile, the maximum stress, σ_m (i.e. the buckling strength), for C2 is 1.57 GPa. Obviously, when $\sigma_P < \sigma < \sigma_m$, the stress increases with the strain, viz. $d\sigma/d\varepsilon > 0$, as shown in Fig. 4a. This stabilizes the deformation of the BMG, like the role of work hardening in crystalline metals [24]. In addition, after reaching a maximum, the stress decreases gradually as the strain increases, never experiencing a

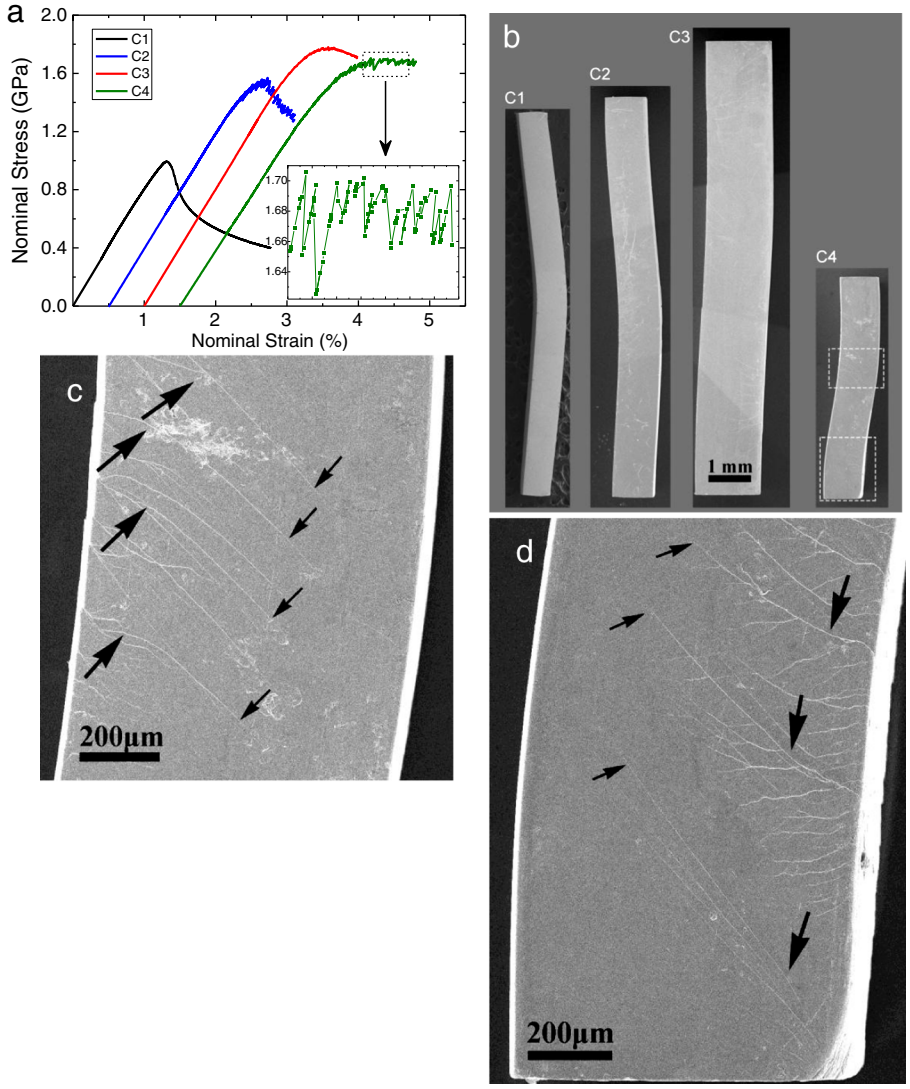

Fig. 4. Plastic buckling behavior of another four slender samples with SR value below 44.4. (a) The compressive stress–strain curves for the samples. The inset shows irregular serrations in the plastic deformation of C4. (b) The SEM profiles of the four buckled samples. The special features of the shear bands can be seen in the middle (c) and at the bottom (d) of C4.

sudden drop. This failure mode is much more benign than brittle fracture. But σ_m is yet to be enhanced to realize the strength potential of BMGs. Therefore, C3 with a smaller SR of 24.6 is compressed. As expected, σ_P and σ_m for C3 increase to 1.74 GPa and 1.77 GPa, approaching σ_y (~1.80 GPa). Moreover, C3 sustains a plastic strain of ~0.5% (see the red curve in Fig. 4a). It demonstrates that the plastic buckling alleviates the brittleness of BMGs at little cost of the strength.

It is known that the compressive plasticity of BMGs strongly depends on the size of the specimen [5,19,25]. To investigate the effect of size on the buckling behavior, another sample C4, about half the length of C3, is tested. Elastic buckling of C4 is, of course, not permitted, which is attributed to the great discrepancy between σ_E listed in Table 1 and σ_y. The green curve in Fig. 4a shows the stress–strain curve of C4. Similar to that of C3, the equilibrium path deviates from the elastic linearity at about 1.6 GPa. Fig. 4b shows the profile of the deformed C4. It is evident that plastic buckling occurs in C4. Accordingly, the buckling behavior of a BMG bar is not influenced by the sample size, but is closely related to the SR value. Furthermore, the shear bands develop in a unique manner during the plastic buckling. Fig. 4c and d show the middle and bottom parts of C4, respectively. It can be seen that multiple shear bands are formed and no regular serrations are found in the plastic deformation regime of C4, as displayed by the inset in Fig. 4a. Hence, the plastic strain is not obtained by sliding along a single primary shear band [13]. Moreover, the propagating paths of all shear bands are not simply straight, but bowed or re-channeled, as marked by the large arrows in Fig. 4c and d. The shear bands never sweep across the sample, and are all blocked midway as marked by the small arrows.

3.4. Universality and practicality of plastic bucklitng in BMGs

For a real slender bar, it begins to deflect, more or less, as soon as the stress is applied due to the bending moment [8]. If the BMG bar is very slender, e.g. B1 or B2, the bending moment remains small until the stress reaches σ_E, so the bent configuration has little influence on the performance [7]. If not very slender, e.g. C3 or C4, the stress becomes large and approaches σ_y before buckling occurs, as shown in Fig. 4a. Because the stress on the concave side of the bent specimen increases more rapidly than on the convex side [7,8], the material on the concave side yields first once the stress reaches σ_y. As a result, the shear bands nucleate there and propagate towards the convex side. Nevertheless, the low stress level on the convex side deters the propagation, so the shear bands are stopped before sweeping across the sample.

As a matter of fact, plastic buckling of a stubby BMG sample is not impossible in compression. Wu et al. [3,18] conducted many compression tests to investigate the geometric effects. They found that 4 of 28 orthogonal BMGs ($Zr_{48}Cu_{45}Al_7$) specimens with aspect ratio of ~2 sustained a noticeable plastic strain beyond 2%, which was ascribed to the specimen's misalignment causing eccentricity of the load. The view point in this paper is that the plasticity mainly comes from the buckling. Most importantly, the misalignment, which can be introduced by the loading or the initial specimen preparation, is more difficult to control, as compared to the SR. The SR value can be altered arbitrarily and precisely by changing dimensions of the sample. In practice, it is feasible to take advantage of the buckling in engineering applications. If the SR is set to a certain value, with which a slender BMG bar buckles plastically at a stress level just below σ_y, optimal performance can be achieved. This value for Zr-based BMGs should range from 20 to 30, as determined in this work.

4. Conclusions

In summary, the BMG is prone to buckle elastically or plastically when its SR value is over about 20. In elastic buckling, the lower buckling strength obliterates the advantage of high strength of the BMG. For plastic buckling, not only is the high strength fulfilled but a benign failure mode is obtained. This mode benefits from the stress gradient which can re-channel and block the propagation of the shear bands. Regarding engineering design, we propose that plastic buckling is superior to the brittle fracture on safety and reliability in BMGs.

Acknowledgments

This work is substantially supported by the Research Grants Council of Hong Kong Special Administration Region (under the project code: PolyU511510). The financial support from the NSF of China (Grant No. 51201001) is also appreciated.

References

[1] C.A. Schuh, T.C. Hufnagel, U. Ramamurty, Acta Mater. 55 (2007) 4067.
[2] Y.H. Liu, G. Wang, R.J. Wang, D.Q. Zhao, M.X. Pan, W.H. Wang, Science 315 (2007) 1385.
[3] W.F. Wu, Y. Li, C.A. Schuh, Philos. Mag. 88 (2008) 71.
[4] M.D. Demetriou, C. Veazey, J.S. Harmon, J.P. Schramm, W.L. Johnson, Phys. Rev. Lett. 101 (2008) 145702.
[5] Z.F. Zhang, H. Zhang, X.F. Pan, J. Das, J. Eckert, Philos. Mag. Lett. 85 (2005) 513.
[6] H. Guo, P.F. Yan, Y.B. Wang, J. Tan, Z.F. Zhang, M.L. Sui, E. Ma, Nat. Mater. 6 (2007) 735.
[7] Z.P. Bažant, L. Cedolin, Stability of structures, World Scientific, Singapore, 2010.
[8] R.M. Jones, Buckling of bars, plates, and shells, Bull Ridge Publishing, Blacksburg, Virginia, 2006.
[9] J.G. Wang, D.Q. Zhao, M.X. Pan, W.H. Wang, S.X. Song, T.G. Nieh, Scripta Mater. 62 (2010) 477.
[10] W.H. Wang, Prog. Mater. Sci. 57 (2012) 487.
[11] M.D. Demetriou, J.C. Hanan, C. Veazey, M.D. Michiel, N. Lenoir, E. Üstündag, W.L. Johnson, Adv. Mater. 19 (2007) 1957.
[12] Z. Bian, M.X. Pan, Y. Zhang, W.H. Wang, Appl. Phys. Lett. 81 (2002) 4739.
[13] S.X. Song, H. Bei, J. Wadsworth, T.G. Nieh, Intermetallics 16 (2008) 813.
[14] A. Niikura, A.P. Tsai, A. Inoue, T. Masumoto, J. Non-Cryst. Solids 159 (1993) 229.
[15] U. Ramamurty, M.L. Lee, J. Basu, Y. Li, Scripta Mater. 47 (2002) 107.
[16] W.F. Wu, Z. Han, Y. Li, Appl. Phys. Lett. 93 (2008) 061908.
[17] H.B. Yu, W.H. Wang, J.L. Zhang, C.H. Shek, H.H. Bai, Adv. Eng. Mater. 11 (2009) 370.
[18] Z. Han, H. Yang, W.F. Wu, Y. Li, Appl. Phys. Lett. 93 (2008) 231912.
[19] Z. Han, W.F. Wua, Y. Li, Y.J. Wei, H.J. Gao, Acta Mater. 57 (2009) 1367.
[20] Y. Yang, J.C. Ye, J. Lu, P.K. liaw, C.T. Liu, Appl. Phys. Lett. 96 (2010) 011905.
[21] Y.Y. Zhao, E. Ma, J. Xu, Scripta Mater. 58 (2008) 496.
[22] R.D. Conner, W.L. Johnson, N.E. Paton, W.D. Nix, J. Appl. Phys. 94 (2003) 904.
[23] L.C. Zhang, F. Jiang, Y.L. Zhao, S.B. Pan, L. He, J. Sun, J. Mater. Res. 25 (2010) 283.
[24] M.A. Meyers, K.K. Chawla, Mechanical behavior of materials, 2nd ed. Cambridge University Press, Cambridge, UK, 2009.
[25] Y.J. Huang, J. Shen, J.F. Sun, Appl. Phys. Lett. 90 (2007) 081919.